

1
2 **Monkeys predict trajectories of virtual prey using basic variables from Newtonian physics**

3
4 Seng Bum M Yoo^{a, b*}, Steven T. Piantadosi^a, and Benjamin Y. Hayden^b

5
6
7 ^aDepartment of Brain and Cognitive Sciences,
8 Center for Visual Science, and
9 Center for the Origins of Cognition
10 University of Rochester,
11 Rochester, NY 14620

12
13 ^bDepartment of Neuroscience and
14 Center for Magnetic Resonance Research
15 University of Minnesota,
16 Minneapolis MN 55455

17
18 **Correspondence:**

19 Seng Bum M. Yoo
20 Department of Neuroscience and
21 Center for Magnetic Resonance Research
22 University of Minnesota,
23 Minneapolis, MN, 55455
24 Email: sbyoo.ur.bcs@gmail.com

25
26 **Short title:** Predicting prey using physics variables

27
28
29
30
31
32
33
34
35
36
37
38
39
40
41
42
43
44

ABSTRACT

The demands of foraging are a major driver in the evolution of cognitive faculties. To successfully pursue a mobile prey that is attempting to avoid capture, the ability to predict its flight path can provide a crucial advantage. We hypothesized that, during pursuit, rhesus macaques exploit patterns in prey's behavior to predict the prey's future positions. We modeled behavior of three macaques in a joystick-controlled pursuit task in which prey follow simple escape algorithms that involve repulsion from the subject and from the walls of the virtual enclosure. We find that, even in this artificial task, macaques actively predict and aim towards prey's future positions, increasing their foraging success. Their predictions are derived from the three core variables in Newtonian dynamics: position, velocity, and acceleration. Even after extensive training, subjects favored these principles and ignored other regularities in prey behavior. Most notably, they ignored the effects their own actions would have on the prey, despite extensive training and even though doing so would have further improved performance. We conjecture that subjects have a strong bias towards using physical principles to pursue fleeing prey, possibly reflecting an evolved physics module. The observed predictive behavior suggests that foraging demands facilitate the development of prospection.

45 **Significant Statement**

46 Real-time prediction is crucial when chasing moving objects. We developed a novel virtual
47 hunting task that requires macaque monkeys to control a joystick to pursue prey continuously
48 moving on a computer screen. We found that subjects actively predict the upcoming position of
49 the virtual prey by taking advantages of basic kinematic principles (speed and acceleration).
50 Their predictions do not reflect expectations about the effects the agent's own actions will have
51 on the prey. These results demonstrate prospection in macaques and also suggest it may have
52 practical limits.

53

INTRODUCTION

54 The demands of foraging are a major driver of our neural and cognitive faculties,
55 including specialized brain systems that allow us to perform complex computations in order to
56 hunt more effectively (1, 2). When faced with mobile prey that move erratically, such as those
57 that are fleeing, the ability to actively predict preys' future positions can provides a boost in
58 pursuit efficiency and, ultimately, survival (3–6). Prediction about the future movements of
59 objects in the environment depends on the ability to calculate future events. It is therefore an
60 element of a suite of skills that constitute prospection - a hallmark of human thought (7, 8).

61 In natural pursuit settings, the ability to predict—rather than simply follow—prey's
62 movement has been shown for some highly specialized species (9), but not primates. Nor are
63 animal prospection abilities strongly established more generally (10–12). Well-known examples
64 of putative animal prospection generally rely on naturalistic foraging contexts, suggesting that it
65 is the need to forage that drives prospective abilities. Nonetheless, such tasks generally operate
66 on the domain of long time scales (often, several days). We conjectured that prey-related
67 prediction should be a much more general skill, and thus be readily observable at short time
68 scales in rapidly changing environments.

69 The manner in which such prospection occurs is poorly understood. Sensorimotor control
70 research shows that humans and animals use inverse models to generate the motor commands
71 that are required to achieve desired sensory states and forward models to predict the sensory
72 outcome of movement (13, 14). Those studies provide hints that prospection might require
73 internal model that simulates predicted outcome. However, such models are limited to self-
74 movement. The types of computations that we use to predict object movement remain

75 unidentified. This problem is compounded when the predicted object adaptively avoids the
76 subject and attempts to elude capture.

77 Here, we developed a virtual pursuit task to test rapid on-line prospection in macaque
78 monkeys with a real-time adaptive pursuit component. The task is loosely inspired by the pursuit
79 of insects, which are thought to be a major driver of primate evolution (15). To determine which
80 strategy the subjects used to capture the prey, we developed a generative framework to model
81 online pursuit movements. The model formalized different possible ways that subject might
82 predict or follow prey, allowing us to quantitatively evaluate what determined subject
83 movements. Our results suggest that macaque monkeys aim their joystick to the position of prey
84 based on extrapolating physical variables of the trajectory, aiming at a position where physics
85 predicts the object is going to be located, even in situations where prey's motion has other
86 regularities.

87

RESULTS

88

89

90

91

92

93

94

95

96

We trained three rhesus macaque subjects on *computerized virtual pursuit task* (subjects K, H, and C). In our task, subjects used a joystick to control the position of an avatar (a yellow circle) moving continuously and smoothly in an open rectangular field on a computer screen (**Fig. 1** and **Methods**). On each trial, subjects had 20 seconds to pursue and capture a prey item (a fleeing colored square) to obtain a juice reward. Prey avoided the avatar with a deterministic strategy that combined repulsion from the subject's current position with repulsion from the walls of the field (see **Methods** for details). One prey was present on each trial; the prey item on any trial was drawn randomly from a set of five, identified by color, that differed in maximum velocity and associated reward size (**Fig. 1**).

97

98

99

100

101

102

103

104

105

All three subjects attained proficiency and showed stabilized behavior within twelve 2-hour training sessions that occurred following an initial longer training period on basic joystick use (see **Fig. S1** and **Fig. S2** for details). All data presented here were collected after the training sessions (number of trials analyzed in this post-training dataset: subject K: 3024; subject H: 3083; subject C: 2512). Subjects successfully captured the prey in over 95% of trials and, on successful trials, did so in an average of 5.04 seconds (subject K: 4.26 sec, subject H: 5.32 sec, subject C: 5.54 sec). Subjects' performance and capture time declined with the maximum speed and reward offered by the prey, indicating sensitivity to manipulation of reward and difficulty (see **Fig. S1**).

106

107

108

109

We next fit the subjects' strategies in pursuing their prey using a generative framework with a small number of parameters. Initially, the framework assumes that subjects exert a force towards either the prey's future position ($\tau > 0$), past position ($\tau < 0$) or current position ($\tau = 0$, **Fig. 2A**) using one of several possible predictive models of the prey's motion. Our primary

110 analyses thus determine (1) the value of the prospection parameter τ , and (2) the performance of
111 different models of the prey's predicted future motion, on each 1-second slice of the predator and
112 prey's motion. Along with τ , the strength of the force applied to the joystick, which in turn
113 quantified the attraction to the prey, was a free parameter fit on each slice.

114 In addition to terms that define the amount of prospection and applied force, we added
115 an inertia term reflecting physical constraints associated with our customized joystick. This
116 inertia term was defined in terms of the velocity of the previous time step. The predicted
117 movement is computed by summing a vector corresponding to the aimed direction and vector of
118 inertia (**Fig. 2**). To compare the difference in fitting result, we calculated the difference of 'the
119 mean for sum-of-squared error' between the model in each trajectory. Thus, if the model with
120 inertia explained specific trajectory better, the value should be negative. We found that in all
121 cases, subjects' performance was better explained by the model having inertia term (**Fig. 3**). For
122 significance testing, we performed bootstrapping for the value we obtained. We still found 5%
123 significance line resulted in a negative value, meaning the negative value obtained in here is
124 significant.

125 To quantify the typical parameter values, we averaged a full grid of parameter values
126 across trajectories, shown in **Fig. 2C**, using a *physics-variable based prediction model* (PVBP)
127 of prey motion (see **Methods**). We observed a strong preference for positive force,
128 demonstrating monkeys are engaging the task. The best fitting τ is positive, indicating that
129 subjects point the joystick towards the prey's future trajectory. This pattern holds for all three
130 individuals tested. Specifically, subjects K, H and C pointed the joystick towards the position at
131 which the prey would be in an average of 800 ms, 767 ms, and 733 ms, in the future respectively.
132 All of these times are significantly greater than zero (more than 95% of bootstrapped data stayed

133 above zero). In the context of the task, these numbers are substantial: they reflect 18.78%,
134 14.42%, and 13.23% of the average trial duration for K, H, and C, respectively.

135 The distance into the future that our subjects prospected did not reliably depend on the
136 reward or the speed of the prey, as measured using a linear regression between reward/speed and
137 mean τ (K: $r = 3.0316$, $p = 0.1110$; H: $r = 4.5798$, $p = 0.1791$; C: $r = 7.1007$, $p = 0.0957$). Prey
138 path complexity (as measured by path curvature) did affect prediction. Subjects prospected less
139 far into the future when the prey path was more complex (K: $\rho = -0.0687$; H: -0.0567 ; C: $-$
140 0.0898 , $p < 0.0001$ for each).

141 We next quantitatively compared possible strategies subjects used to predict future prey
142 direction by formalizing different computations by which monkeys could predict future
143 trajectories (**Fig. 2A**) and fitting the parameters to each. The *veridical prediction (VP) algorithm*
144 assumes that monkeys predict according to the true game dynamics in which prey move away
145 from the boundaries of the field and also from the avatar. The *cost contour map prediction*
146 (*CCMP*) *algorithm* matches VP but ignores repulsion from the avatar, meaning that monkey's
147 model of prey would not take into account their own motion. Third, the *physics variable-based*
148 *prediction (PVBP) algorithm* assumes that subjects' predictions derive from the prey's position
149 and first two derivatives, velocity and acceleration (additional derivatives are considered in **Fig.**
150 **S3**). We measured the accuracy of each algorithm by computing the predicted path of the subject
151 on every trajectory slice then computing its error (sum of squared distance between predicted and
152 observed trajectories).

153 We use the Akaike Information Criterion (AIC) to compare models (**Fig. 4** and
154 **Methods**). This figure shows that the PVBP model of future prey trajectories is overall the best
155 fit to our subjects' behavior. This pattern held within the two well-trained subjects. Specifically,

156 the *PVBP algorithm* was favored (Subject K: PVBP: 7.529×10^6 , second best was VP: 7.542×10^6 ;
157 Subject H: PVBP: 8.923×10^6 ; second best was CMPP: 8.950×10^6 , **Fig. 4A**). For the less well-
158 trained subject C, *CCMP* explained trajectories most accurately (7.955×10^6 , VP: 8.013×10^6).
159 These patterns appear to be robust to the specific analysis as they could be seen in also by
160 estimating which model fit best for each individual trajectory slice (**Fig. 4B**).

161 Because Subject C showed a different pattern, and Subject C performed worst overall
162 (and thus chased slower prey), we wondered whether prey speed may influence strategy.
163 Supporting this idea, a trial-by-trial logistic regression between whether PVBP was the best
164 model and average prey velocity showed a positive relationship for all three subjects ($p < 0.01$ in
165 each case), with subject C maintaining a similar proportion of trajectories best explained by
166 PVBP for its speed (**Fig. S5**). These results highlight the adaptive flexibility of prospective
167 pursuit strategy selection, and indicate that Subject C's overall difference can be explained by
168 the relatively slower speed prey used.

169 We asked which values of parameters are closest to optimal in capturing prey using
170 simulations (**Fig. 5**). To exclude the possibility where optimal parameters exist beyond what
171 subjects can accomplish using the current joystick configuration, we examined optimality by
172 comparing performance under identical pursuit/inertia ratios, which can be accomplished by
173 limiting the range of the force parameter in simulation. The representative prediction parameter
174 in simulation shows that all subjects' prediction parameter sets are not identical to the optimal
175 parameter set obtained from PVBP simulation. Average capture time in simulation using optimal
176 parameter was 1.10 second while top 5% capture time of actual trial was 1.31 second (subject
177 K), 1.32 second (subject H). The value of the optimal prediction parameter was 335 pixels
178 compare to actual prediction of each animal was 536 (subject K), 455 (subject H) pixels (Subject

179 C's prediction is not directly comparable in pixel units because the prey in simulation had
180 maximum speed matched with subject K and subject H but faster than subject C's game). These
181 results suggest that our subjects' pursuit strategy is less than the optimal even subject to
182 reasonable empirically derived constraints, and performance would have improved once they
183 used shorter prediction scales.

184

DISCUSSION

185

186

187

188

189

190

191

192

193

194

We trained macaques to perform a novel joystick-based pursuit task. The generative framework we developed to model our subjects' strategies shows that macaque monkeys do not simply point the joystick towards the prey, but actively predict its future position. Notably, they extended basic principles of Newtonian physics to this artificial situation. That is, each subject's movement is best explained by a model that predicts prey position based on extrapolating variables derived from physics (velocity and acceleration). These results therefore show that, in a difficult dynamic pursuit context, macaques will rapidly and naturally take advantage of regularities in their prey's behavior to gain an advantage in reward intake. Moreover, they show that our subjects demonstrate a basic ability to perform the necessary computations to predict future prey positions and to exploit that prediction.

195

196

197

198

199

200

201

202

Our generative framework does not explain why animals prefer using basic physical principles and ignoring other factors that could make their predictions more accurate. One possibility is that the brain is equipped with a physics module that performs mental simulation about the physics of external environment (16). By having a module that specifically simulates physics, computations for external physics change would be more efficient than reasoning about underlying method how prey movement is generated. The fact that animals favor the physics predictions in the most difficult cases – those with the fastest prey – provides at least suggestive evidence for the idea that the physics based approach is one that is more natural.

203

204

205

206

Our results provide support, in a very different form than other studies, for the idea that our brains simulate physics to making judgement of the scene, sometimes called 'intuitive physics' (17–20). Previous studies related to intuitive physics have mainly focused scene understanding or moving objects without any interactions between the subject participant and the

207 stimulus. Our study expands on these previous findings by generalizing for cases where
208 environment changes dynamically and interactively.

209 More broadly, our results open a unique direction to understand real-time pursuit
210 behavior. The majority of the behavioral studies try to use minimally simple tasks that sacrifice
211 naturalness in order to control each variable precisely to understand behaviors. Such tasks can
212 cause behavior to enter into modes that are unnatural. On the other hand, real-time naturalistic
213 behavior requires frameworks to narrow down hypothesis space. Our study has set example of
214 studying real-time dynamic behavior under guidance of well-established framework.

215 Questions about prospection aside, the ability to make choices based on expectations of
216 future events is a basic skill in the repertoire of intelligent decision-makers (21–23). Those
217 abilities guide appropriate selection of choices in foraging contexts, including under both risk
218 and delay (24–26). A unique factor of our study is its focus on real-time decisions, that is,
219 decisions in which subjects choose from a continuum of possible actions - which constitute a
220 corresponding continuum of options - and reassess their options as their actions occur (27–30).
221 Some scholars have argued that these types of decisions are the type of decisions that drove the
222 evolution of our choice systems (2, 31, 32). As such they provide a more realistic assessment of
223 choice behavior than binary choice tasks. We anticipate that future studies using this paradigm
224 and others like it will lead to greater insight into the psychological and neural mechanisms of
225 choice.

226

MATERIALS AND METHODS

227

Subjects Three male rhesus macaques (*Macaca mulatta*) served as subjects in the current

228

experiment. All animal procedures were approved by the University Committee on Animal

229

Resources at the University of Rochester and were designed and conducted in compliance with

230

the Public Health Service's Guide for the Care and Use of Animals.

231

Experimental Apparatus The joystick was a modified version of commercially available

232

joysticks with a built-in potentiometer (Logitech Extreme Pro 3D). The control bar was removed

233

and replaced with a control stick (15 cm, plastic) designed to be ergonomically easy for

234

macaques to manipulate. The joystick position was read out by a custom coded program in

235

Matlab running on the stimulus-control computer. The joystick was controlled by detecting the

236

positional change of the joystick and limiting the maximum pixel movement to within 23 pixels

237

in 16.66 ms.

238

Task Design At the beginning of each trial, two shapes appeared on a gray computer

239

monitor placed directly in front of the macaque subject. The yellow (subject K) and purple circle

240

(subject H and C) shape (15-pixel diameter) represents the subject himself and its position is

241

determined by the joystick and limited by the screen boundaries. The square shape (30-pixel

242

length) represents the prey. The movement of the prey is determined by a simple AI (see below).

243

Each trial ends with either successful capture of the prey or after 20 seconds, whichever comes

244

first. Successful capture is defined as any overlap between the avatar circle and the prey square.

245

Capture results in immediate juice reward; juice amount corresponds to prey color: orange (0.3

246

mL), blue (0.4 mL), green (0.5 mL), violet (0.6 mL), and cyan (0.7 mL).

247

The path of the prey was computed interactively using A-star pathfinding methods, which

248

are commonly used in video gaming (33). For every frame (16.66 ms), we computed the cost of

249 15 possible future positions the prey could move to in the next time-step. These 15 positions
250 were spaced equally on the circumference of a circle centered on the prey's current position, with
251 radius equal to the maximum distance the prey could travel within one time-step. The cost in turn
252 is computed based on two factors: the position in the field and the position of the subject's
253 avatar. The field that the prey moves in has a built-in bias for cost, which makes the prey more
254 likely to move towards the center (**Fig. 1B**). The cost due to distance from the subject's avatar is
255 transformed using a sigmoidal function: the cost becomes zero beyond a certain distance so that
256 the prey does not move, and the cost becomes greater as distance from the subject's avatar
257 decreases. Eventually, the costs from these 15 positions are calculated and the position with the
258 lowest cost is selected for the next movement. If the next movement is beyond the screen range
259 (1920x1080 resolution), then the position with the second lowest cost is selected, and so on.

260 The maximum speed of the subject was 23 pixels per frame (i.e. 16.66 ms). The
261 maximum and minimum speeds of the prey varied across subjects and were set by the
262 experimenter to obtain a large number of trials (**Fig. 1**). Specifically, speeds were selected so that
263 subjects could capture prey on above 85% of trials; these values were modified using a staircase
264 method. If subjects missed the prey three times consecutively, then the speed of the prey was
265 reduced. Once the subject intercepts the prey in a trial where the staircase method was used, then
266 the selection of prey speed was randomized again. To ensure sufficient time of pursuit, the
267 minimum distance between the initial position of each subject avatar and prey was 400 pixels.

268 ***Behavioral Model*** To fit each subject's movement, each trial was divided into 1 second-
269 long trajectories and each trajectory included 61 data-points with 16.66 ms time resolution. We
270 model these trajectories using a single prediction and a single force parameter for the entire trial,
271 as a simplifying assumption. Nonetheless, it is reasonable to assume that throughout a long, 20-

272 second period, there would be active adjustment of prediction and force. Actual comparison by
273 AIC supported our intuition, and we used trajectory as unit of analysis throughout (value of ‘AIC
274 of trajectory/AIC of trial’ was 0.9328, 0.9214, 0.9227, for each subject respectively. Less than
275 one indicates trajectory as unit result in better fitting).

276 The model assuming Physics Variable-Based Prediction (PVBP) incorporated one
277 previous time step to predict the prey’s next position, which is like a Kalman filter. The other
278 two models do not utilize any past information. The model assuming prediction using the cost
279 contour map considers only the lowest cost location at next time step. The model assuming
280 veridical prediction automatically finds the exact position of the prey at the next time step. Once
281 the prey’s position on the next time step is predicted, the model computes how far this predicted
282 position is from the agent’s current position. A prediction value of 1 indicates that the future
283 position will be as far as from the agent’s current position as the prey’s current position is. The
284 optimal parameter pairs of how much subject has made prediction and actual amount of force
285 was acquired by performing a grid search across the ranges of both parameters. The range of the
286 prediction parameter was between -400 to 400 subjects H and C, -200 to 200 for subject K (units
287 were defined relative to the distance the prey moved in the previous timestep). Different ranges
288 of the prediction parameter were used since over 5% of trajectories in subjects H and C resulted
289 either in -200 or 200 in prediction parameter value. Representative parameters for explaining an
290 each trajectory were selected based on the value of the sum of squared error between the actual
291 trajectory and the trajectory generated by model.

292 ***Significance Testing*** To see whether the positive prediction parameter is significant
293 above the zero, we performed a bootstrap of heatmap slices from each trajectory. This

294 resampling was done for 500 times and selected heatmaps were added. Then, the parameter set
295 resulting in the lowest cost was selected in each resampling.

296 ***Model Evaluation*** To evaluate model performance and compare different models, we
297 computed the Akaike Information Criteria (AIC) using the likelihood of each model (**Fig. 4, and**
298 **Fig. S3, Fig. S4**). For calculating likelihood, we first calculated the mean and variance of all the
299 sum-of-squared errors across trajectories. Then we estimated the likelihood assuming a normal
300 distribution centered on the mean of the sum-of-squared errors and with a variance equivalent to
301 the variance of the sum-of-squared errors across all trajectories. To validate whether subjects
302 used a single prediction and force across the all the trials or adaptively changed their prediction
303 method, we compared the AIC value between cases where the parameter pair varied across all
304 trajectories and using only the single best parameter pair. The single best parameter pair is
305 acquired by lowest cost value in all trajectory added heatmap of parameter space.

306 ***Simulation*** To estimate the efficiency of parameter values obtained from fitting subjects'
307 behavior, we performed a simulation with 100 different initial positions of artificial subjects and
308 prey (**Fig.5**). The algorithm generating prey movements was the same as that used in the actual
309 task, and the movements of the artificial subject were generated based on different prediction
310 methods. The maximum duration for each simulation was 1200 time-bins, which is equivalent to
311 20 seconds (the longest possible trial in the actual task). All the values of the parameter sets
312 (prediction, force) that were used for fitting actual behavior were simulated.

313 ***Velocity Dependent Physics Variable-Based Prediction Bias*** We examined whether
314 PVBP is preferred when the velocity of prey is high. We first obtain the average velocity of prey
315 at each trajectory, and then categorized each trajectory as physics variable-based prediction if the
316 fitting result was best with physics variable-based prediction and non-physics when other

317 prediction method provided the best fitting result. With the prey velocity and trajectory category,
318 we performed logistic regression having velocity as predictor and category as the dependent
319 variable (glmfit in MATLAB).

320 ***Data availability*** The data sets generated during the current study are available on the
321 Hayden lab website, <http://www.haydenlab.com/>, or from the authors on reasonable request. The
322 code generated to do the analyses for the current study is available from the corresponding
323 author on reasonable request. Video of experiment is available at
324 <http://www.haydenlab.com/pursuit>.

325 **Acknowledgements**

326 We thank Habiba Azab, Steve Chang, and John Pearson for the valuable discussions and
327 comments in manuscripts. We are grateful for Haydenlab and CoLaLa lab for intuitive
328 discussion that has lead into elaborating the model classes. We appreciate Marc Mancarella and
329 Giuliana LoConte for advising the training monkeys, Alex Thome for developing method, and
330 Shannon Cahalan for helping data collection. This work was supported by the NIH R01
331 DA038615 for B.H.Y.

332

333 **Authors Contribution**

334 S.B.M.Y. and B.Y.H. designed the study. S.B.M.Y. trained monkeys and collected data. S.P. and
335 S.B.M.Y develop the behavioral model, analyzed the data and model outcome. B.Y.H., S.P. and
336 S.B.M.Y. wrote the manuscript.

337

338 **Competing interests statement**

339 The authors declare that they have no competing financial interests.

340

341 **Correspondence** and request for the materials should be address to S.B.M.Y

342 (sbyoo.ur.bcs@gmail.com)

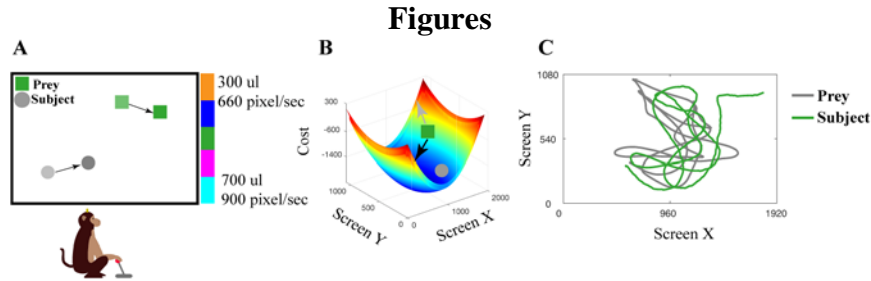
343

Reference

- 344 1. Passingham R, Wise S (2012) *The Neurobiology of the Prefrontal Cortex* (Oxford
345 Scholarship Online).
- 346 2. Pearson JM, Watson KK, Platt ML (2014) Decision making: The neuroethological turn.
347 *Neuron* 82(5):950–965.
- 348 3. Catania KC (2009) Tentacled snakes turn C-starts to their advantage and predict future
349 prey behavior. *Proc Natl Acad Sci* 106(27):11183–11187.
- 350 4. Catania KC (2010) Born knowing: Tentacled snakes innately predict future prey behavior.
351 *PLoS One* 5(6): 1–10.
- 352 5. Borghuis BG, Leonardo A (2015) The role of motion extrapolation in amphibian prey
353 capture. *J Neurosci* 35(46):15430–15441.
- 354 6. Mischiati M, et al. (2015) Internal models direct dragonfly interception steering. *Nature*
355 517(7534):1–13.
- 356 7. Suddendorf T, Corballis MC (2007) The evolution of foresight: What is mental time
357 travel, and is it unique to humans? *Behav Brain Sci* 30(3):299–351.
- 358 8. Schacter DL, Addis DR, Buckner RL (2007) Remembering the past to imagine the future:
359 the prospective brain. *Nat Rev Neurosci* 8(9):657–661.
- 360 9. Wiederman SD, Fabian JM, Dunbier JR, O’Carroll DC (2017) A predictive focus of gain
361 modulation encodes target trajectories in insect vision. *Elife* 6:1–19.
- 362 10. Clayton NS, Bussey TJ, Dickinson A (2003) Opinion: Can animals recall the past and plan
363 for the future? *Nat Rev Neurosci* 4(8):685–691.
- 364 11. Raby CR, Clayton NS (2009) Prospective cognition in animals. *Behav Processes*
365 80(3):314–324.
- 366 12. Roberts WA (2002) Are animals stuck in time? *Psychol Bull* 128(3):473–489.
- 367 13. Wolpert DM, Ghahramani Z, Jordan MI (1995) An internal model for sensorimotor
368 integration. *Science* 269:1880–1882.
- 369 14. Franklin DW, Wolpert DM (2011) Computational mechanisms of sensorimotor control.
370 *Neuron* 72(3):425–442.
- 371 15. Strier KB *Primate Behavior Ecology*. Taylor & Francis (Routledge, 5th edition).
- 372 16. Fischer J, Mikhael JG, Tenenbaum JB, Kanwisher N (2016) Functional neuroanatomy of
373 intuitive physical inference. *Proc Natl Acad Sci* 113(34):5072–5081.
- 374 17. Battaglia PW, Hamrick JB, Tenenbaum JB (2013) Simulation as an engine of physical
375 scene understanding. *Proc Natl Acad Sci* 110(45):18327–18332.
- 376 18. Ullman TD, Spelke E, Battaglia P, Tenenbaum JB (2017) Mind Games: Game Engines as
377 an Architecture for Intuitive Physics. *Trends Cogn Sci* 21(9):649–665.
- 378 19. Kubricht JR, Holyoak KJ, Lu H (2017) Intuitive Physics: Current Research and
379 Controversies. *Trends Cogn Sci* 21(10):749–759.
- 380 20. Sanborn AN, Mansinghka VK, Griffiths TL (2013) Reconciling intuitive physics and
381 Newtonian mechanics for colliding objects. *Psychol Rev* 120(2):411–37.
- 382 21. Polnaszek TJ, Stephens DW (2013) Why not lie? Costs enforce honesty in an
383 experimental signalling game. *Proc R Soc B Biol Sci* 281(1774).
- 384 22. Winstanley CA, Dalley JW, Theobald DEH, Robbins TW (2004) Fractioning impulsivity:
385 Contrasting effects of central 5-HT depletion on different measures of impulsive
386 behaviour. *Neuropsychopharmacology* 29(7):1331–1343.
- 387 23. Santos LR, Rosati AG (2015) The Evolutionary Roots of Human Decision Making. *Annu*
388 *Rev Psychol* 66(1):321–347.

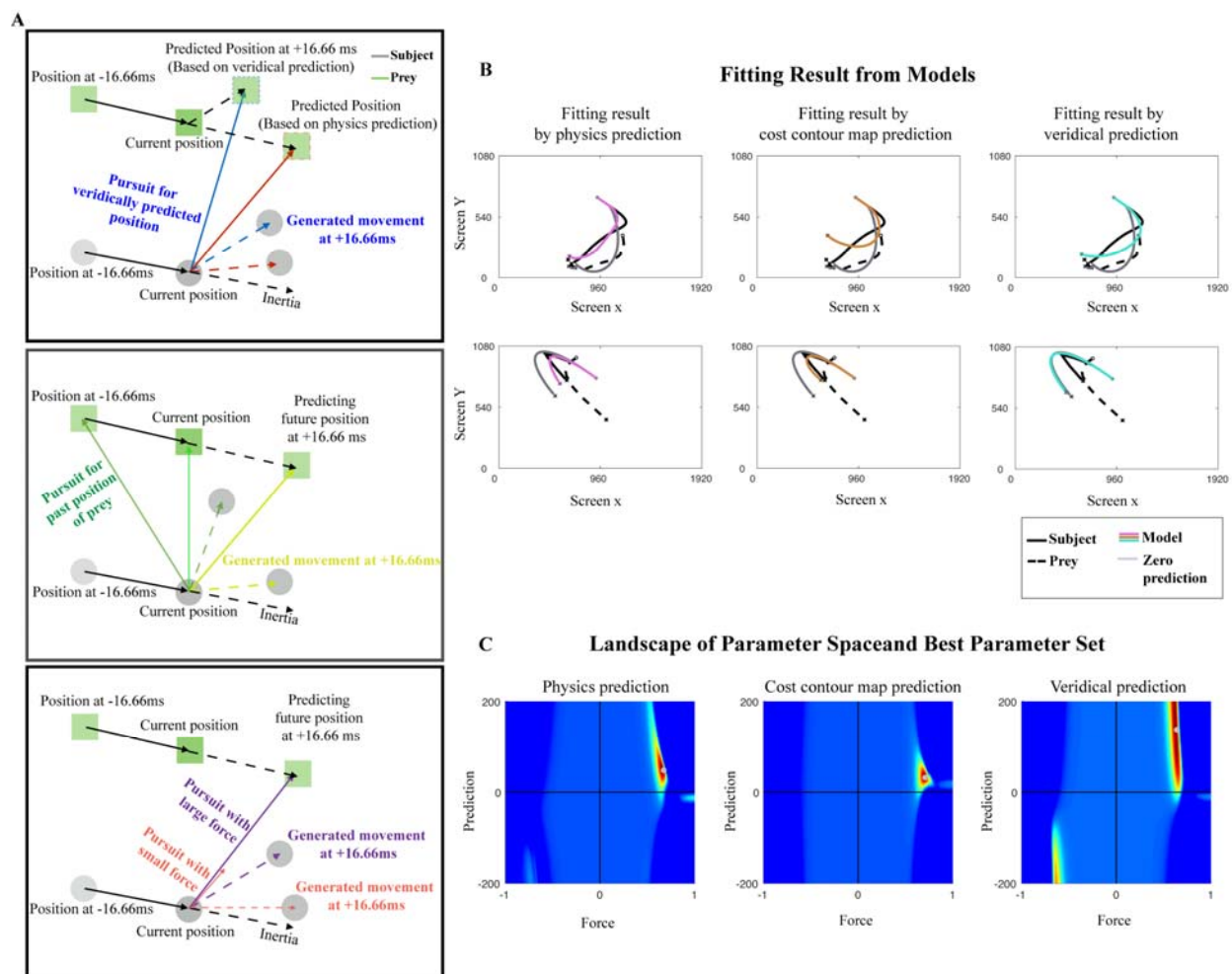
- 389 24. Blanchard TC, Hayden BY (2015) Monkeys are more patient in a foraging task than in a
390 standard intertemporal choice task. *PLoS One* 10(2):1–11.
- 391 25. Blanchard TC, Wilke A, Hayden BY (2014) Hot-hand bias in rhesus monkeys. *J Exp*
392 *Psychol Anim Behav Process* 40(3):280–286.
- 393 26. Hayden BY (2016) Time discounting and time preference in animals: A critical review.
394 *Psychon Bull Rev* 23(1):39–53.
- 395 27. Cisek P (2012) Making decisions through a distributed consensus. *Curr Opin Neurobiol*
396 22(6):927–936.
- 397 28. Resulaj A, Kiani R, Wolpert DM, Shadlen MN (2009) Changes of mind in decision-
398 making. *Nature* 461(7261):263–266.
- 399 29. Kiani R, Cueva CJ, Reppas JB, Newsome WT (2014) Dynamics of neural population
400 responses in prefrontal cortex indicate changes of mind on single trials. *Curr Biol*
401 24(13):1542–1547.
- 402 30. Wehrhahn C, Poggio T, Bühlhoff H (1982) Tracking and chasing in houseflies (*Musca*) -
403 An analysis of 3-D flight trajectories. *Biol Cybern* 45(2):123–130.
- 404 31. Cisek P, Pastor-Bernier A (2014) On the challenges and mechanisms of embodied
405 decisions. *Philos Trans R Soc London B Biol Sci* 369(1665):1–14.
- 406 32. Pezzulo G, Cisek P (2016) Navigating the Affordance Landscape: Feedback Control as a
407 Process Model of Behavior and Cognition. *Trends Cogn Sci* 20(6):414–424.
- 408 33. Hart PE, Nils J (1968) Formal Basis for the Heuristic Determination of Minimum Cost
409 Path. *IEEE Trans Syst Sci Cybern* 4(2):100–107.
- 410

411

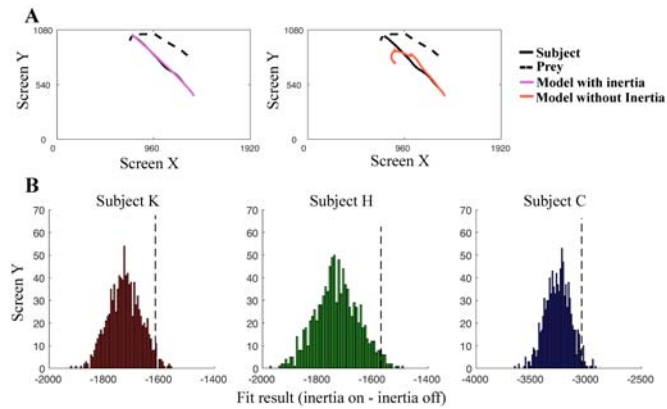


412

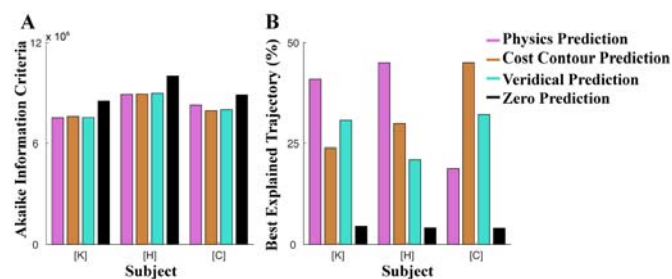
413 **Fig. 1.** Experimental design. (A) Cartoon illustrating the virtual pursuit task. A subject moves a
414 joystick to control the position of an avatar (yellow circle). The task code determines the prey's
415 next position according to the movement of the subject and the built-in cost contour map (in
416 panel B). Updates of both subject and prey positions occur every 16.66 ms, (i.e. 60 Hz: identical
417 to screen refresh rates). (B) The cost contour map across the screen. At each time-step, the task
418 code determines the prey's next move by choosing the position with the lowest cost. Cost is
419 higher as prey moves closer to the edges and corners of the screen (to prevent the prey from
420 being cornered by the predator). The configuration of this cost-contour map makes the prey more
421 likely to move (1) away from the subject (grey arrow), and (2) towards the center of the screen
422 (black arrow). (C) Example trajectories (capture time: 7.84 seconds). Green trajectory indicates
423 the subject's actual trajectory, while the grey trajectory indicates the prey's actual trajectory.



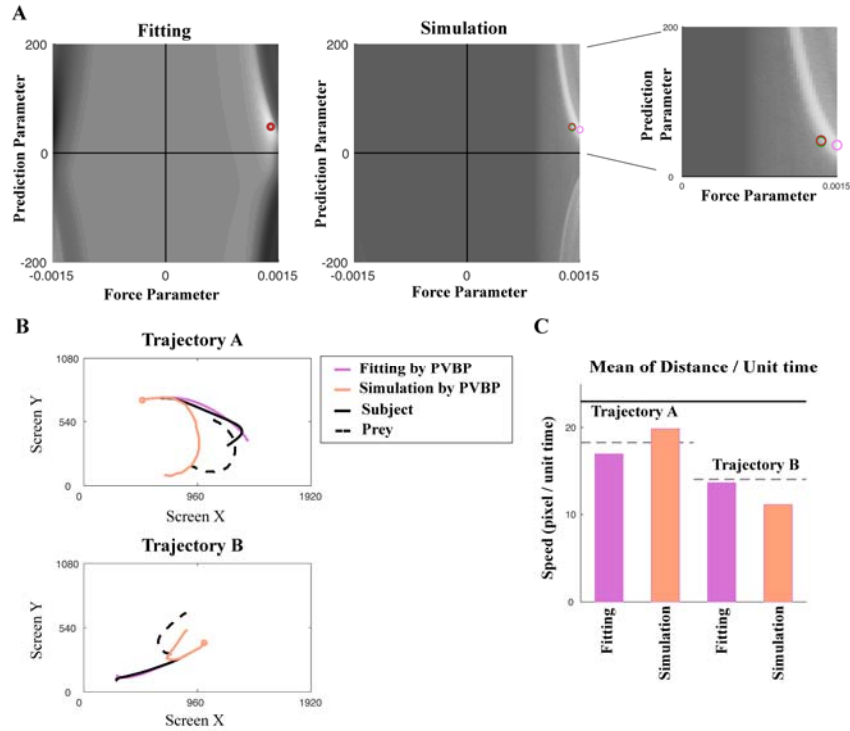
424
 425 **Fig. 2.** Model description, fitting results for single trial and population. **(A)** Model to generate
 426 trajectory based on prediction. Solid black arrow indicates movement from one previous time
 427 point (i.e. 16.66 ms before) to the current time point. The prediction for the prey's position at the
 428 next time point is generated according to each model type. The monkeys are assumed to aim at a
 429 point forwards or backwards along the predicted trajectory, as determined by tau. The resulting
 430 movement vectors are constrained to a maximum speed specific to each subjects' motor
 431 constraints. **(B)** Two example trajectories (left and right columns), and the fit trajectory
 432 generated by each prediction method (Physics Variable-Based, Cost Contour Map, and
 433 Veridical). The empty circle in the trajectory indicates the starting position, and the star marker
 434 indicates the ending position of the trajectory. **(C)** Heatmap plots of model performance
 435 explaining subject's pursuit trajectory across parameter space from a single subject (Subject K).
 436 The gray circle indicates the best parameter combination explaining subject's behavior, which
 437 generates the closest distance between the actual trajectory and model-predicted trajectory.



438
439 **Fig. 3.** Inertia enhances model performance. (A) Model trajectory comparison between models
440 with and without inertia. (B) Histogram results suggest that incorporating inertia component to
441 the model leads to a better fit of the data (mean for sum-of-squared error difference below zero at
442 x-axis). 95% of data falls to the left of the black, dashed line. Bootstrapping of difference in
443 performance between the model with and without inertia was performed in randomly sampled
444 trajectories (number of resamples: 1000, randomly selected trajectories: 2000).



445
446 **Fig. 4.** The fitting result across the subjects and model comparison. (A) Normalized Akaike
447 Information Criteria (AIC) across all the trajectories. In the current figure, only the Physics
448 Variable-Based Prediction (PVBP) based on velocity and acceleration is included as
449 representative of all the physics variable-based prediction models. (B) Percentage of trials best
450 explained by each model. The AIC values are compared across models.



451
452 **Fig. 5.** Pursuit trajectory of monkey is less than optimal compare to simulation result. (A) Left
453 column is heatmap of fitting trajectory (identical as Fig. 2C, gray scaled for showing subject's
454 best parameter in color) and right column is capture time result from simulating artificial subject.
455 Pink circle indicates best parameter obtained from simulation and other circles is best parameter
456 from fitting each subject (red: Subject K; green: Subject H; subject C was not included since
457 simulation matched prey speed with Subject K and H). (B) Trajectories generated by using best
458 parameter from fitting (pink) and best parameter from simulation (light orange). The results
459 suggest different strategy selection according to parameter (Quantitative comparison for
460 capturing time between simulation and actual monkey's behavior is at supplementary results).
461 (C) Mean of distance per unit time in given example trajectory. Black line is maximum distance
462 per unit time possible and gray dashed line is the mean of actual subject's distance per time.
463 Fitting parameter results in smaller value for trajectory A while has larger value for trajectory B.

464

SUPPLEMENTARY MATERIALS

465 *Pseudocode for Pacman Game Algorithm*

466 prey_size = 30 pixel

467 number_of_angle = 15

468 distance_factor = 50

469 time_out = 20 seconds (resolution: 60Hz: 1200 data points)

470 weight_x = sigmoidal function between 0 and 1920

471 weight_y = sigmoidal function between 0 and 1080

472 cost_grid = [1920 x 1080 matrix: z-axis is shown in **Fig.1B**]

473

474 index = 1

475 **While** prey_capture or time_out

476 % subject position is joystick input (x_coordinate, y_coordinate).

477 % initial position: randomly selected.

478 % prey_position is arbitrary random value.

479 % initial position: 400 pixel away from subject initial position.

480 prey_away_vector = prey_pos - subj_pos;

481 normalized_away_vector = prey_away_vector/sqrt(sum(prey_away_vector²));

482

483 % Multiple weight vector: If farther than particular distance, prey will not move.

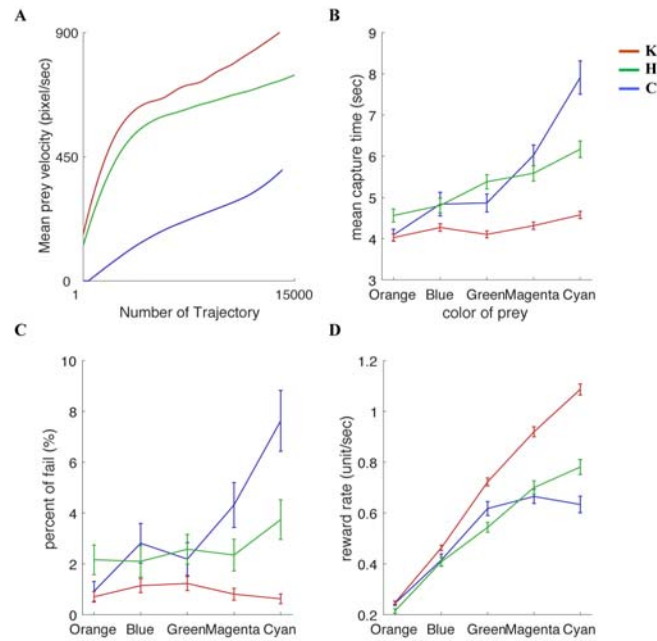
484 normalized_away_vector(1) = normalized_away_vector *weight_x;

485 normalized_away_vector(2) = normalized_away_vector *weight_y;

486

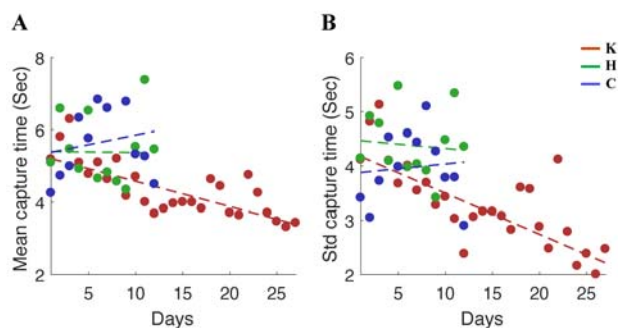
```
487     % multiply speed of prey: vary 5 levels
488     speed_considered_vector = normalized_away_vector*prey_speed;
489
490     % Compare 15 different positions: same distance, different angle.
491     For number_of_angle
492         rotation_matrix = [cosd(angle), -sind(angle); sind(angle), cosd(angle)];
493         rotated_away_vector = rotation_matrix * speed_considered_vector;
494         potential_prej_pos = current_prej_position + rotated_away_vector;
495
496         % Calculate distance related value
497         dist_from_subject = sqrt( sum( potential_prej_pos - current_subj_pos)^2 )
498         dist_points = distance_factor *dist_from_subject;
499
500         % cost according to shape of cost grid: how does imaginary screen look like
501         grid_points = cost_grid( potential_prej_pos(x), potential_prej_pos(y));
502
503         % value considered for final movement
504         final_cost = dist_points + grid_points;
505     Endfor
506
507     % check condition whether prey is captured
508     If sqrt( sum( potential_prej_pos - current_subj_pos)^2 ) <= prey_size then
509         prey_capture = True;
```

```
510     Endif
511
512     % check timeout
513     If index == time_out
514         time_out = True;
515     else
516         % update index
517         index = index +1;
518     Endif
519 Endwhile
```

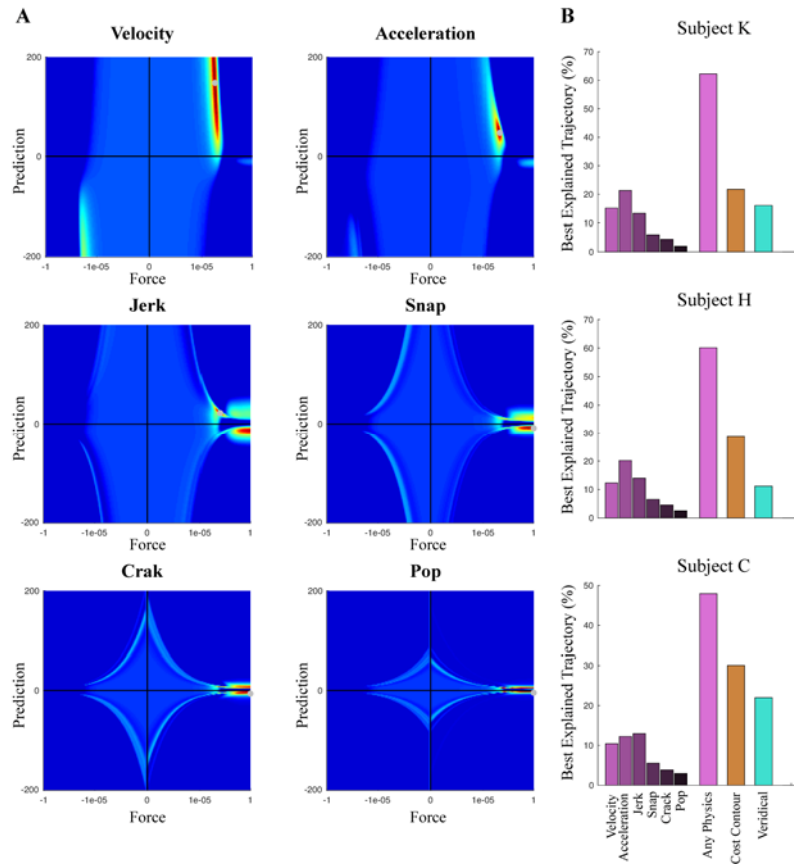


520

521 **Fig S1.** Monkeys behavior varies according to prey speed/reward. (A) Mean prey velocity in each
522 trajectory plotted separately for each subject. Pursuit result differs according to color (equivalent to
523 maximum speed) of prey. The maximum speed of prey increases from orange (slowest with smallest
524 reward) to cyan (fastest with largest reward). As maximum speed increases, the mean capturing time (B)
525 and percent of failed trials increase (C). However, reward rate also increases since the amount of reward
526 is larger for faster prey (D). Errorbars are the standard error of the mean, obtained by bootstrapping
527 (1000 bootstraps).



528
529 **Fig S2.** Stabilization of the behavioral performance. Performance stabilization shown by the mean (**A**)
530 and the standard deviation (**B**) of prey capture time. Subject C (blue) and Subject H (green) do not show
531 any significant changes in their capture time throughout the days of the experiment (linear regression with
532 p -value > 0.1) while Subject K (red) shows significant changes to both mean and standard deviation of
533 capture time across days (p -value < 0.001).



534

535 **Fig S3.** Second order approximation of physics explains trajectory most accurately. (A) Each

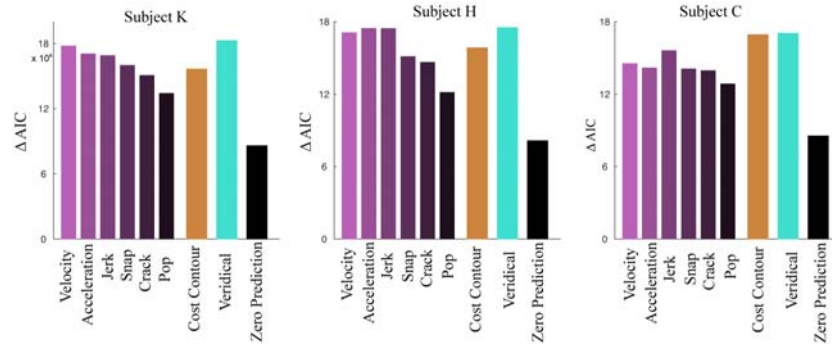
536 heatmap indicates the addition of more physical derivatives until sixth derivatives. The black

537 circle indicates the best parameter set for the model. (B) In summary figure, physics include

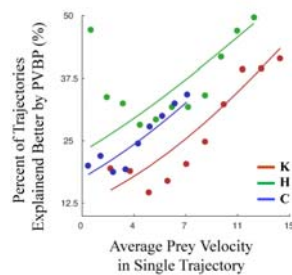
538 within-physics prediction model comparison (from velocity to pop, the 6th derivative). Any

539 physics indicate summed result of whole physics variable based prediction (PVBP) model class

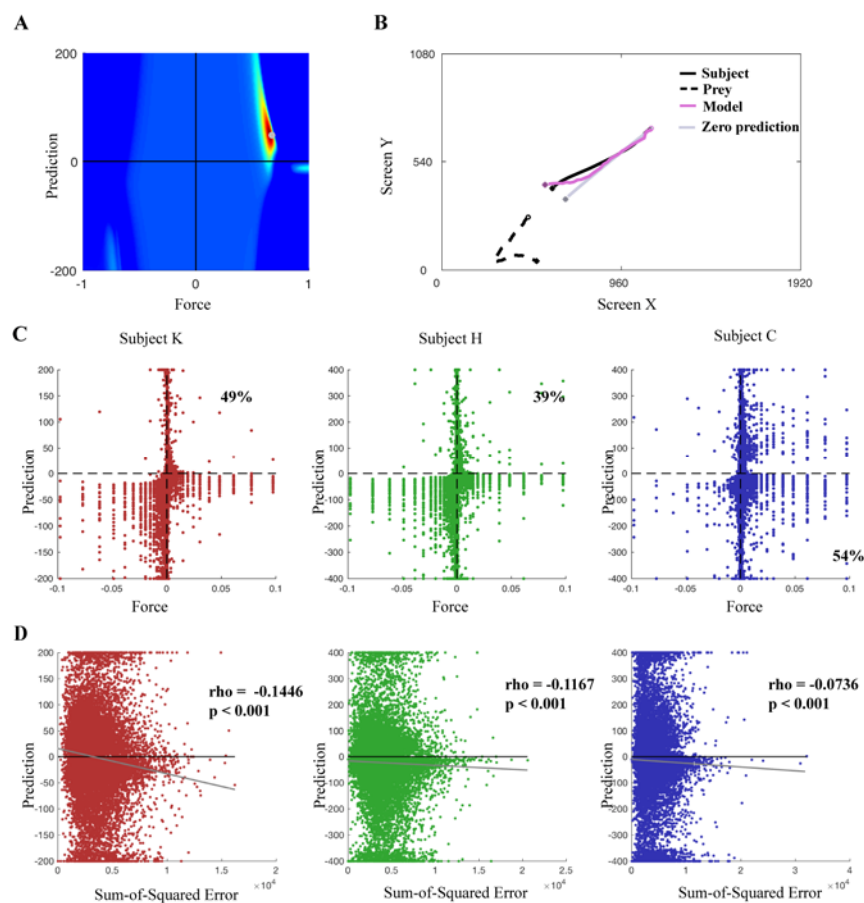
540 to compare with other prediction methods.



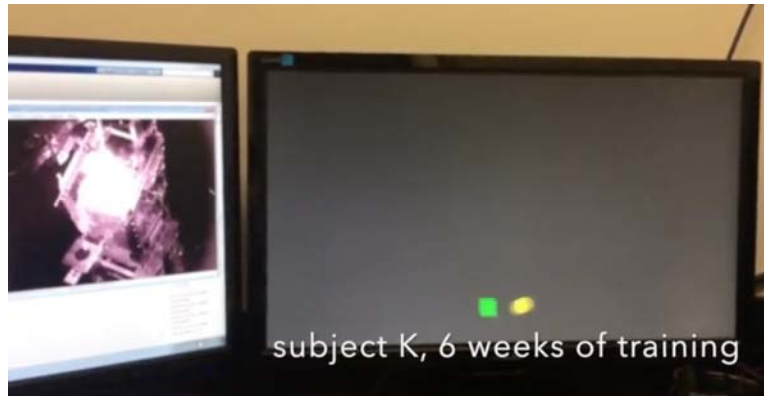
541
542 **Fig S4.** Dynamic change of parameter set at each trajectory explains monkey's trajectory better
543 than identical single parameter set across all the trajectories. AIC comparison between the case
544 of the single parameter set across all the session (case 1) or adaptively changing parameter set at
545 each trajectory (case 2). Delta AIC indicates the difference between the cases (case 1 - case 2),
546 and a positive value indicates adaptively changing the strategy explains subject's trajectory better
547 even there is penalty having more parameters. Each column shows the individual subject result.



548
549 **Fig S5.** Prey velocity dependent strategy selection. All the monkeys consistently show biases
550 using PVBP when the prey velocity is faster. Logistic regression was performed between prey
551 velocity and categorical dependent variable (0: non-PVBP, 1: PVBP). The p-values of all logistic
552 coefficient was significant ($p < 0.001$).



553
 554 **Fig S6.** Some trajectories explained with negative prediction. (A) Though the representative
 555 parameter set appears at positive prediction and positive force (identical figure as PVBP heatmap
 556 at figure 2C, across all trajectory heatmap). (B) Some trajectories are better explained with
 557 negative prediction, as indicated by an example trajectory. The model trajectory in (B) results
 558 from PVBP with ‘velocity and acceleration accounted’. (C) The fitting of individual trajectory
 559 displayed as scatter plot. Percent indicates the most fitting resulted in that quadrant (subject K
 560 and H: 1st quadrant with both positive prediction and force; subject C: 4th quadrant with positive
 561 force and negative prediction). (D) Scatter plot and polynomial fitting (grey solid line) result for
 562 cost against prediction. The rho and p-values are obtained from Spearman rank correlation. This
 563 provides reason for positive prediction in all subjects: method of heatmap accounts how well
 564 each trajectory is fitted.



565

566 **Movie 1.** Video of two primates subject playing dynamic pursuit task. Each subject was filmed in
567 different stage of training (subject K: 6 weeks after initial joystick training, subject C: 3 weeks after initial
568 joystick training).